Mechanism and Machine Theory 86 (2015) 1–14

Contents lists available at ScienceDirect

Mechanism and Machine Theory

journal homepage: www.elsevier.com/locate/mechmt

Speed losses in V-ribbed belt drives

Berna Balta [a,b], Fazil O. Sonmez [c,*], Abdulkadir Cengiz [d]

[a] Department of Mechanical Engineering, Kocaeli University, Kocaeli, Umuttepe, 41380, Turkiye
[b] Ford Otosan, Product Development Department, Kocaeli, Gebze 41470, Turkiye
[c] Department of Mechanical Engineering, Bogazici University, Istanbul, Bebek, 34342, Turkiye
[d] Mechanical Education Department, Kocaeli University, Kocaeli, Umuttepe, 41380, Turkiye

ARTICLE INFO

Article history:
Received 11 December 2013
Received in revised form 10 November 2014
Accepted 24 November 2014
Available online xxxx

Keywords:
V-ribbed belt drives
Slip
OFAT
RSM
Design optimization
ANOVA

ABSTRACT

One of the concerns in belt drive transmissions is the relative sliding (slip) of the belt with respect to the pulley, which results in speed loss, i.e. decrease in the angular velocity of the driven pulley. In this study, the slip behavior of a V-ribbed belt drive with two equal-sized pulleys is investigated by utilizing several experimental methodologies. The individual effects of belt-drive parameters on speed loss are determined using one-factor-at-a-time (OFAT) test method. The relation between the belt-drive parameters and the speed loss is found using response surface method (RSM). Afterwards, the optimum operating conditions are determined via a design optimization procedure. In order to validate the response surface curve, experiments are conducted with arbitrary operating conditions and the measured and predicted values of speed loss are compared. The predictions of the response surface model are also found to be in good agreement with the empirical results presented in the literature. Furthermore, the predicted model looks reasonably accurate based on the analysis of variance (ANOVA) and the residual analysis. Using the response curve, one may estimate the degree of speed loss for similar belt-drives with operating conditions within the range considered in the present study.

1. Introduction

Belt drives are power transmission systems commonly used in the industry [1]. There are different types of belts like flat belts, V-belts, and V-ribbed belts. Flat belts offer flexibility, while V-belts offer high power transmission capacity. V-ribbed belts, on the other hand, combine these two properties. They are made of a layer of reinforcing cords as tension-carrying members, a protective cushion of rubber that envelopes the cords, a rubber backing, and ribs made of short-fiber-reinforced rubber as shown in Fig. 1.

In comparison to the traditional V-belts, V-ribbed belts have numerous advantages including accommodation to smaller pulleys sizes and belt lengths, backside operation, and relatively longer service life. The ribs on V-ribbed belts guide the belt and make it more stable in comparison to the traditional flat-belts; they also provide increased power transmission capacity by increasing the friction surface and normal pressure.

High efficiency and high performance of V-ribbed belt drives can only be achieved if proper values are chosen for the design parameters. This requires fundamental understanding of the operational characteristics unique to this class of belts and belt drive systems. High efficiency can be achieved by decreasing power losses. In belt drives, power losses occur due to a combination of speed losses and torque losses [1]. Speed losses result from sliding of the belt relative to the pulley, which leads to a decrease in the angular velocity of the driven pulley, and thus in the transmitted power. With a proper design of belt drives, power losses can

* Corresponding author. Tel.: +90 212 359 7196.
E-mail addresses: bguner@ford.com (B. Balta), sonmezfa@boun.edu.tr (F.O. Sonmez), akcengiz@kocaeli.edu.tr (A. Cengiz).

http://dx.doi.org/10.1016/j.mechmachtheory.2014.11.016
0094-114X/

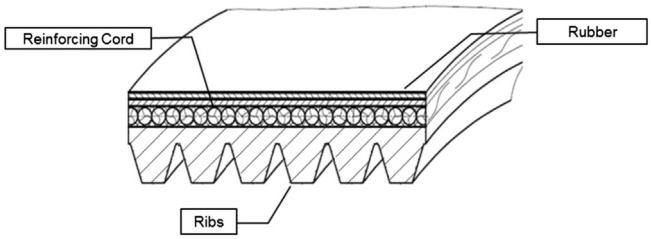

Fig. 1. A scheme for V-ribbed belts.

be decreased and, thus, their efficiency can be increased; but this requires fundamental understanding of the effects of the dominant factors on power loss.

Some researchers theoretically examined the slip behavior in belt drives. In 1874, Reynolds showed that torque transmissions between pulleys involved speed losses due to belt's elastic creep [2]. Gerbert [3] explained the mechanism of slipping by dividing the arc of contact between belt and pulley into sticking (non-slipping) and slipping regions. The belt was treated as a string and the mechanism of elastic creep of the belt along the pulley was shown to yield a slip arc at the exit region of the pulley, where the entire transition from the high to low tension occurred. In the remaining contact region, commonly referred to as the stick (non-slip) arc, the belt was shown to stick to the pulley without slipping with no change in tension [4]. Although the classical creep theory explains how belt slip occurs to a reasonable extent, speed losses encountered in practice are larger than predicted by extensional creep, particularly for thick flat-belts, V-belts, and V-ribbed belts. Firbank [5] proposed a theory where shear strain in the belt envelope was assumed to be the determining factor on the drive behavior. The difference between the two theories is that the creep theory assumes that belt behavior is governed by the elastic extension and contraction of the belt as opposed to the shear theory. However, both of the assumptions are too strict to explain the slip behavior and the slip regions along the contact region between the belt and the pulley. Firbank claimed that slip occurred only at the exits of the driver and driven pulleys. The remaining region over the entire arc was taken as the real arc of contact as defined by Gerbert [6]. Gerbert [7] proposed an analysis that considered both flexural rigidity and compressibility of the belt and assumed that belt speed differences in the entry and exit regions were observed due to the change in the radius of the curvature of the belt, which meant that belt extensibility was not the only factor to explain the slip behavior. Sorge etal. [8] defined the arc of contact as the power transmitting part of the belt and claimed that there was almost no tension variation in the contact region.

Previous experimental studies on power loss behavior of belt drives usually considered V-belt drives and continuously variable transmission (CVT) belt drives. Researchers basically used belt drive test setups with two equal-sized-pulleys. Peeken and Fischer [9] developed a V-belt drive test setup to determine the efficiency up to 200 Nm torque and 6000 rpm speed with a fixed shaft distance. The belt pre-tension was provided by a pivoted rocking arm. They obtained braking torque vs. slip relation for a single combination of belt tension, belt length, and pulley diameter.

Childs and Cowburn [10] experimentally investigated the effects of mismatch between the wedge angles of pulley grooves and belt ribs on the power loss behavior of V-belt drives. During the tests, they kept the other parameters constant. They [11] also studied the effects of small pulleys on the power loss both theoretically and experimentally. Using pulleys with diameters ranging from 42 mm up to 102 mm, they examined the effect of braking torque on power loss. In the experiments, the same belt length and belt material were used.

Lubarda [12] analytically formulated the variation in the belt force over the arc of contact of flat and V-belts before gross slip occurs. He separated the arc of contact into active and non-active regions, similar to the approach of Gerbert [3] and Johnson [4].

A number of studies were conducted to investigate CVT type belt drives used in motorcycles with the help of two-pulley-belt drive test rigs. Ferrando et al. [13] developed a test setup to determine the effects of the drive parameters on the axial force. A velocity controller was used to maintain its speed. By means of electric motors, the driver pulley was actuated and braking torque was applied to the driven pulley. The belt tension, the input torque, and the total axial force in the belt were measured. With a similar setup, Amijma et al. [14] studied the effects of acceleration or deceleration on the power transmission behavior of a CVT belt drive by measuring the axial force via a load cell at a constant speed (2430 rpm) and a constant braking torque. Chen et al. [15] focused on the efficiency of a rubber V-belt CVT drive. In the test setup, input and output torques were measured by torque transducers and speed was measured by optical encoders. Additionally, they installed laser displacement sensors in order to detect the changes in the pitch radii of CVT pulleys and determined the speed and torque losses under different operating conditions. Akehurst et al. [16–18] investigated the power transmission efficiency of a metal V-belt CVT drive. The belt was constructed from several hundred segments held together by steel band sets. They formulated the torque loss and belt-slip losses and correlated them with the experimental results. Bertini et al. [19] studied the power losses in a rubber V-belt type CVT, both experimentally and analytically. They grouped the power loss contributors as hysteresis losses and frictional losses arising at the entrance and exit regions of the pulleys due to engagement/disengagement of the belt. They validated their model through a test bench, which was capable of measuring the transmitted torques, axial trusts on the pulleys, pulley speeds, and belt tension. However, they did not use different belts and pulley diameters to evaluate their effects. Mantriota [20–22] performed extensive experiments to study the efficiency of power-split CVT (PS-CVT). PS-CVT was obtained by joining a V-belt CVT, a planetary gear train, and a timing belt. Input and output angular speeds and torques were measured by means of torque-tachometers integrated to the driving and driven shafts. A regulation

valve controlled pneumatic disk brake was used to apply output torque [20,21,23]. The efficiency of the PS-CVT system was shown to be notably higher than simple CVT systems [20–22]. A detailed experimental investigation concerning the dynamics of a metal pushing V-belt CVT was conducted by Carbone et al. [24]. They compared the theoretical predictions of Carbone–Mangialardi–Mantriota (CMM) model [25] with the experimental results. They equipped their test rig with sensors to measure pressure, rotational speed, and pulley-sheave position [24]. In another study, Zhu et al. [26] experimentally measured power losses in a rubber V-belt CVT for a low-power vehicle like scooters and snowmobiles.

The previous studies considered only flat belt, V-belt, and V-belt CVT drives before V-ribbed belt drives were introduced in the last decades. For this reason, the published papers on V-ribbed belt drives are relatively few [27–36]. Dalgarno et al. [27] developed a V-ribbed-belt-drive test setup with two-pulleys to investigate gross slip-born audible noise. A motor and a generator were installed to provide driver and driven pulley torque loads. The input torque was monitored using an in-line torque transducer. An idler tensioner was used to provide and maintain the belt pre-tension. Also, encoders and a tension transducer were used to measure the speed and belt tension, respectively. They tested three different types of belts with the same geometrical profile. The noise levels of these belts were compared at different operating conditions.

Yu et al. [28] developed a two-pulley V-ribbed belt drive system running at 1000 rpm. They applied different levels of braking torque and measured the radial position of the belt in the pulley grooves by placing laser displacement sensors over the arc of the driver and driven pulleys. Yu [29] investigated the parameters affecting mechanical performance of a two-pulley belt drive system by using four different belts: a new cut belt, a used cut belt, molded belt, and anti-wear belt. Yu et al. [30] also investigated wearing patterns of V-ribbed belts.

Misalignment is another important issue in belt-drive systems. Xu et al. [31] used a simple static two-pulley test setup for the assessment of lateral forces in misaligned pulleys driving a V-ribbed belt. A dead weight was hanged to one of the pulleys to induce initial tension and the results obtained under static conditions were correlated with FEA results.

In another V-ribbed belt drive study, Manin et al. [32] investigated the effects of different types of front-end accessory drive (FEAD) tensioners on the belt span vibration and pulley-belt slip. They constructed a four-pulley-belt drive system, including a driver pulley actuated by an electric motor, a driven pulley, and two idler pulleys; one of which was a tensioner. The speeds of the driver, driven, and tensioner pulleys were measured via encoders, and a laser sensor was also installed to detect belt flapping. Belt pre-tension was measured by a piezo-electric sensor. Driving and driven torques were measured via strain gages. They obtained the relation between the slip and the braking torque for three different tensioner types (idler, hydraulic, and dry friction) and two different low speed levels, 280 and 840 rpm, while keeping the other parameters constant. They also measured the belt slip for two different levels of belt tension using one type of belt tensioner.

Cepon et al. [33] studied the effects of contact parameters, i.e. the friction coefficient, normal contact force, and tangential belt velocity. They measured the belt-pulley contact stiffness and the friction coefficient on two different specific test setups. They also constructed a two-pulley V-ribbed belt drive test setup, where the angular speeds of the driver and driven pulleys were measured using two optical encoders. The driving and braking torques were measured by torque transducers. A hydraulic pump was used to apply braking torque to the belt drive system. Their study was limited to a single combination of belt type, belt length, and pulley size.

Cepon et al. [34], measured the longitudinal stiffness, transverse stiffness, and bending stiffness of V-ribbed belts on a test rig with two equal-sized pulleys. In another test rig, they measured the first three natural frequencies of the V-ribbed belt via displacement sensors. They did not study power losses. In the same test rig, Cepon and Boltezar [35] measured the speed losses and longitudinal vibrations of the belt at its tight and slack sides using two displacement sensors. They concluded that because analytical formulations depended on the creep theory and neglected the radial and tangential deformations of the belt, analytical results were obtained to be far below the experimental ones.

Pietra and Timpone [36] built up a test rig with two-equal-sized pulleys in order to measure the tension ratio between the tight and slack sides of the belt. They used a dead weight to tension the belt drive and mounted strain gages on the outer surfaces of the belt to measure the belt tension. They compared their measurements with theoretical results. By using a high speed camera, they also measured the slip of a thick V-belt.

In order to minimize slip, Kumar and Sooryaprakash [37] developed a closed loop controlled belt tensioner. The slack and tight side tensions were measured by means of displacement sensors. The belt tension was maintained at a predetermined value by the tensioner controller, which adjusted the belt tension based on the sensor signals.

Analytical formulations of slip and torque loss were presented previously for flat and V-belt drives: Gerbert [38] analyzed slip and torque loss in V-belt drives considering the radial compliance and flexural rigidity. Gerbert [3] then derived another analytical formula for the speed loss of thick flat belts. He accounted for shear deflection, radial compliance, and seating/unseating behavior. Later on, Gerbert [7] extended the analytical slip formulation with a unified approach for flat and V-belts based on the creep theory. Belofsky [39] presented a new formulation for the tension ratio of the tight and slack sides by considering the belt elasticity, flexural rigidity, and variation of friction force along the contact arc. Childs and Cowburn [11] proposed a new formulation for the speed loss and torque loss behaviors of V-belt drives. They accounted for belt bending stiffness, radial compliance, pulley diameter, and belt pre-tension.

Several studies conducted finite element analyses of flat and V-ribbed belts. Chen and Shieh [40] obtained the speed loss in a flat belt transmission system by developing a 3D finite element model. Yu et al. [41] constructed a 3D finite element model in order to calculate the radial positioning of a V-ribbed belt into the pulley grooves.

There are several studies [3–11,38,40] on the slip behavior of flat and V-belt drives. Few studies [27–29,32,34,35] exist on the slip behavior of V-ribbed belt drives. In those studies, a limited number of belt drive parameters were considered. The effect of belt length has not been studied.

In the present study, the effects of the belt-drive parameters on the speed loss behavior of V-ribbed belt drives are experimentally investigated. For this purpose, a test setup is constructed with two equal-sized pulleys to measure the speed losses in a V-ribbed belt drive system. In comparison to the previous studies, a much larger number of parameters and their interactions are taken into consideration; they include belt tension, driver pulley speed, braking torque, belt length, pulley diameter, and belt material. The effects of the belt length on the speed loss of V-ribbed belt drives are investigated for the first time. After building the setup, a measurement system analysis (MSA) is conducted in order to ensure the precision and repeatability of the measured data. Then, the effects of the individual parameters are determined using one-factor-at-a-time (OFAT) testing methodology. Furthermore, using response surface methodology (RSM), the relation between the input parameters and the speed loss is obtained. Finally, optimum operating conditions are determined for minimum speed loss via an optimization procedure.

2. Experimental study

2.1. Experimental setup and instrumentation

In this study, the setup shown in Fig. 2 and schematically depicted in Fig. 3 is built to investigate the effects of various parameters on the speed loss behavior of V-ribbed belt drives. J-type V-ribbed belts with four ribs are used to transmit power between the pulleys. The belt drive is actuated by an electric motor having a maximum power output of 3 kW. A frequency inverter is used to control the angular velocity of the driver pulley. Braking torque is applied to the driven pulley by means of a hydraulic pump, which serves as a dynamometer. It can be run at different steady state operating conditions by adjusting a valve; in this way, different levels of braking torque can be provided. The maximum braking torque capacity is 10 N.m. The controllable input parameters and the measured parameters are given in Table 1.

In order to be able to modify the belt tension and accommodate different pulley diameters and belt lengths, the motor is placed on a sliding base. Pre-tension is induced in the belt by means of a spring mechanism, which can apply different levels of force to the sliding base. The total axial force in the belt is measured by a load cell. The dynamometer is mounted on ball bearing housing. The magnitudes of the reaction forces causing torque are measured by the load cell mounted on the housing. In this study, neglecting the frictional torques, the torque calculated using the measured values of force at the housing is assumed to be equal to the braking torque directly applied by the dynamometer. The angular speeds of the driver and driven pulleys are measured with two optical encoders. Additionally, a photoelectric switch is installed to count the belt rotation. A linear variable differential transformer (LVDT) sensor is placed next to the driver pulley to detect the radial displacement of the belt into the pulley grooves under tension. In order to measure the central distance between the pulleys, a dial gage is placed to the sliding base on which the motor is mounted. The data measured by the encoders, photoelectric switch, load cells, and LVDT are processed in the microprocessors to be converted to digital data; then they are transferred to the computer using a data acquisition software, LabVIEW™.

2.2. Measurement system analysis (MSA)

MSA is performed at the beginning of an experimental study to ensure that the information collected is a true representation of what is occurring in the experiment. Experimental data collected under the same conditions usually show variation, which arises

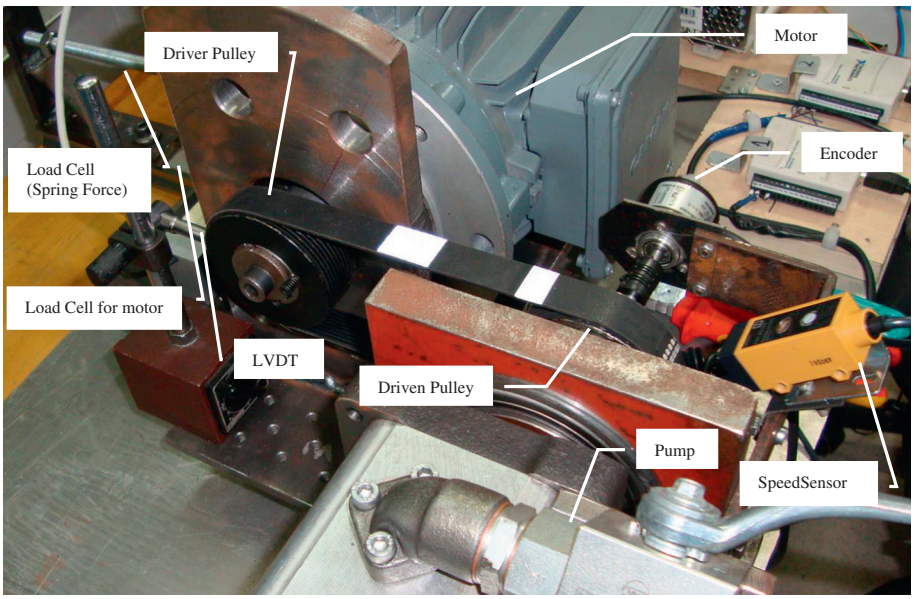

Fig. 2. The experimental setup.

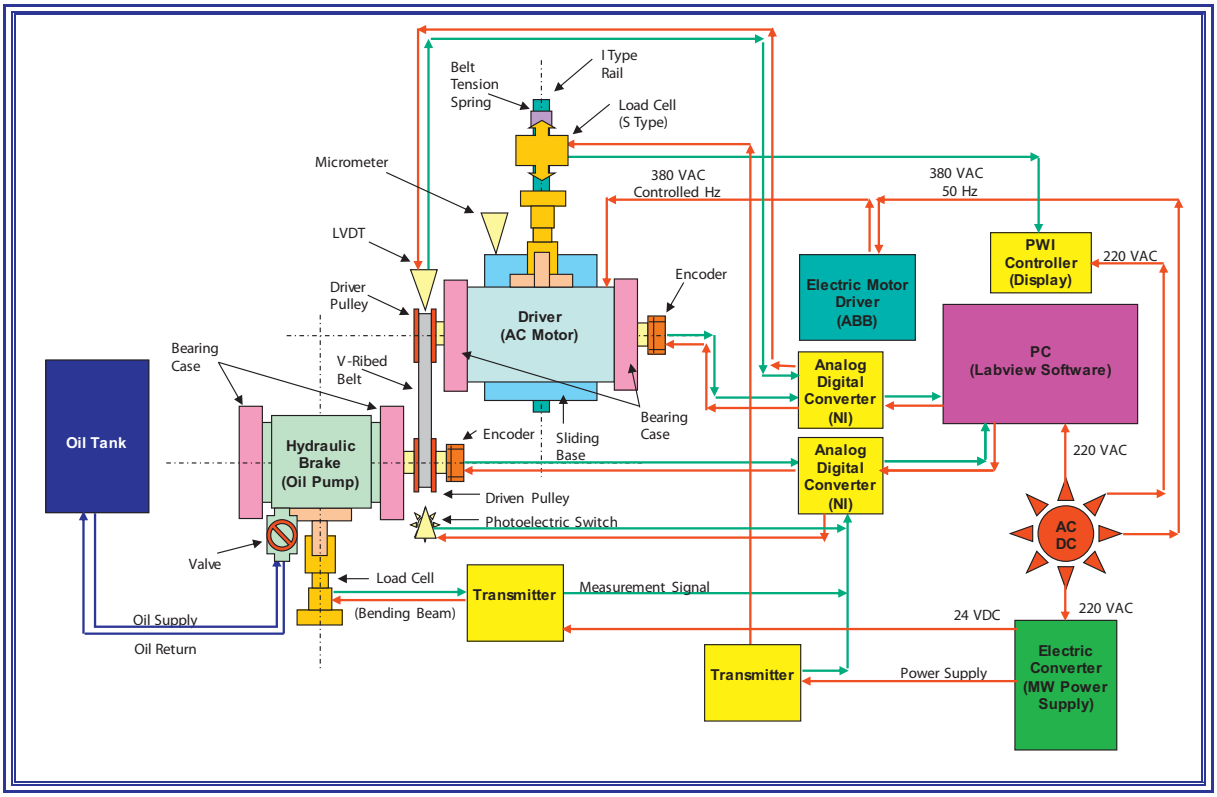

Fig. 3. Schematic of the experimental setup and the instruments.

partly from the experimental system and partly from the measurement devices. MSA helps to differentiate the contribution of these sources to the randomness of the data. In this way, one may see whether there is a need to reduce the measurement variation so that the data reflect basically the experimental variation. Besides, MSA gives quantitative measures for repeatability and reproducibility. Repeatability is the variation in repeated measurements taken by the same measurer under the same experimental conditions. Reproducibility is the variation in data obtained by different measurers taking the measurement with the same setup under the same conditions. These are measures for the consistency and precision of data [42–44].

Gage Repeatability and Reproducibility (GR&R) is the most commonly used measurement system analysis tool to examine the viability of an experimental setup. Resultant GR&R will indicate an overall measurement system variation as the sum of repeatability variation and reproducibility variation. Generally, GR&R % gives a measure of the suitability of the measurement system to yield acceptable data for statistical studies such as design of experiments (DoE), OFAT, and response surface [43–45].

In this study, MSA tests are performed under 5 N.m braking torque and 510 N belt pre-tension using 72.5 mm-diameter pulleys and a belt having 559 mm length and J-type geometry. The elastic modulus of the belt is measured to be 2.5 GPa. These parameters correspond to the standard operating conditions of a FEAD system in a vehicle. Only the motor speed is changed, while the other parameters are kept constant. The driver-pulley speed is altered starting from 866 rpm up to 2030 rpm with 291 rpm increments, and the speed losses (slip) are measured via encoders. Five experiment conditions are tested with three replicas by two operators.

The data are analyzed in Minitab and the results are presented in Tables 2 and 3, where the sum of squares (SS) is the sum of squared distances or amount of variability in the data due to different sources. Degree of freedom (DF) is associated with each SS.

Table 1
The test parameters.

System input parameters	System measured parameters
Motor speed	Pulleys' angular speeds
Braking torque	Braking torque
Belt pre-tension	Belt pre-tension
Belt length	Belt length
Pulley diameter	Belt speed
Belt material	Center distance

Table 2
Analysis of variance (ANOVA) for the MSA study.

Source	DF	SS	MS	F	P
Experiment	4	35.8637	8.9659	2414.523	0.000
Operator	1	0.0986	0.0986	26.5566	0.007
Experiment∗operator	4	0.0148	0.0037	2.2922	0.095
Repeatability	20	0.0324	0.0016		
Total	29	36.0096			

In general, DF measures how much independent information is available to calculate each SS. Mean squares (MS) takes into account the fact that different sources have different numbers of levels or possible values. An F-value shows whether the effects of operator, experiment, or operator × experiment significantly influence the measurement. % contribution parameter gives the ratio of the variance of a component to the total variation; precision-to-total-variation parameter (P/TV) gives the ratio of the standard deviation of a component to the total standard deviation. Total GR&R % contribution and P/TV % are obtained to be 0.58% and 7.59%, respectively. These values denote that 0.58% of the total measured variance is from repeatability and reproducibility of the experimental setup, and 7.59% of the spread of variability is estimated as coming from the measurement system.

These metrics all confirm that the measurement system is valid, i.e. it can be used in a DoE or response surface study. According to the criteria of the Automotive Industry Action Group for gage acceptance [43,44], an experimental system that has a contribution % less than 1.0% and variation less than 10% is considered as an ideal system.

2.3. Measuring speed losses

After installing the V-ribbed belt onto the pulleys, the sliding bases are pulled apart until a specific belt tension is created. The driver pulley, rotated by the motor, actuates the belt, which in turn rotates the driven pulley, while the dynamometer applies braking load to the belt-drive system. Due to relative sliding between the belt and the pulleys, a difference arises between the speeds of the driver and driven pulleys. This is called speed loss, which will be referred to as "slip" from now on, evaluated by the following equation for two equal-sized pulleys:

$$\%\ Slip = \frac{\omega_{driver} - \omega_{driven}}{\omega_{driver}} \times 100 \tag{1}$$

where ω_{driver} and ω_{driven} are the rotational speeds of the driver and the driven pulleys, respectively.

In the setup, the angular speeds of the pulleys are measured using two optical encoders. Based on these measured data, the slip is calculated. In order to verify the encoder measurements, the belt speed is also measured by means of a photoelectric switch, which counts the passes of light reflecting tapes bonded on the outer surface of the belt. Linear belt speeds are then converted into rotational speeds over the arc of contact. The maximum error, which is the difference between the encoder and photoelectric switch measurements of the driver pulley speed, is calculated as 0.8%.

2.4. One-factor-at-a-time (OFAT) test results

The individual effects of the belt-drive parameters on % slip losses are first determined by conducting tests in which one parameter is changed at a time. Elastic modulus is assumed to be the only property of the belt material that affects slip behavior. Accordingly, the elastic modulus is directly taken as a belt drive parameter. The results are shown in Fig. 4.

In Fig. 4a, slip losses are shown as a function of braking torque applied to the driven pulley. Increasing braking torque significantly increases the slip. This effect is more pronounced at low levels of pre-tension and speed. In Fig. 4b, slip losses are given as a function of driver pulley speed. Slip (%), which is defined as $100 \times \Delta\omega/\omega_{driver}$, remains nearly constant for different levels of driver pulley speed except at low levels of pre-tension and high braking torque. Note that absolute rotational speed differences, $100 \times \Delta\omega$, rise via increase

Table 3
The results of GR&R study [42].

Source	Variance Component	% Contribution	St. dev	% P/TV
Total GR&R	0.0086	0.58	0.0930	7.59
Repeatability	0.0016	0.11	0.0402	3.28
Reproducibility	0.0070	0.47	0.0838	6.84
Operator	0.0063	0.42	0.0795	6.49
Experiment∗operator	0.0007	0.05	0.0264	2.16
Experiment-to-experiment	1.4937	99.42	1.2222	99.71
Total variation	1.5024	100.00	1.2257	100.00

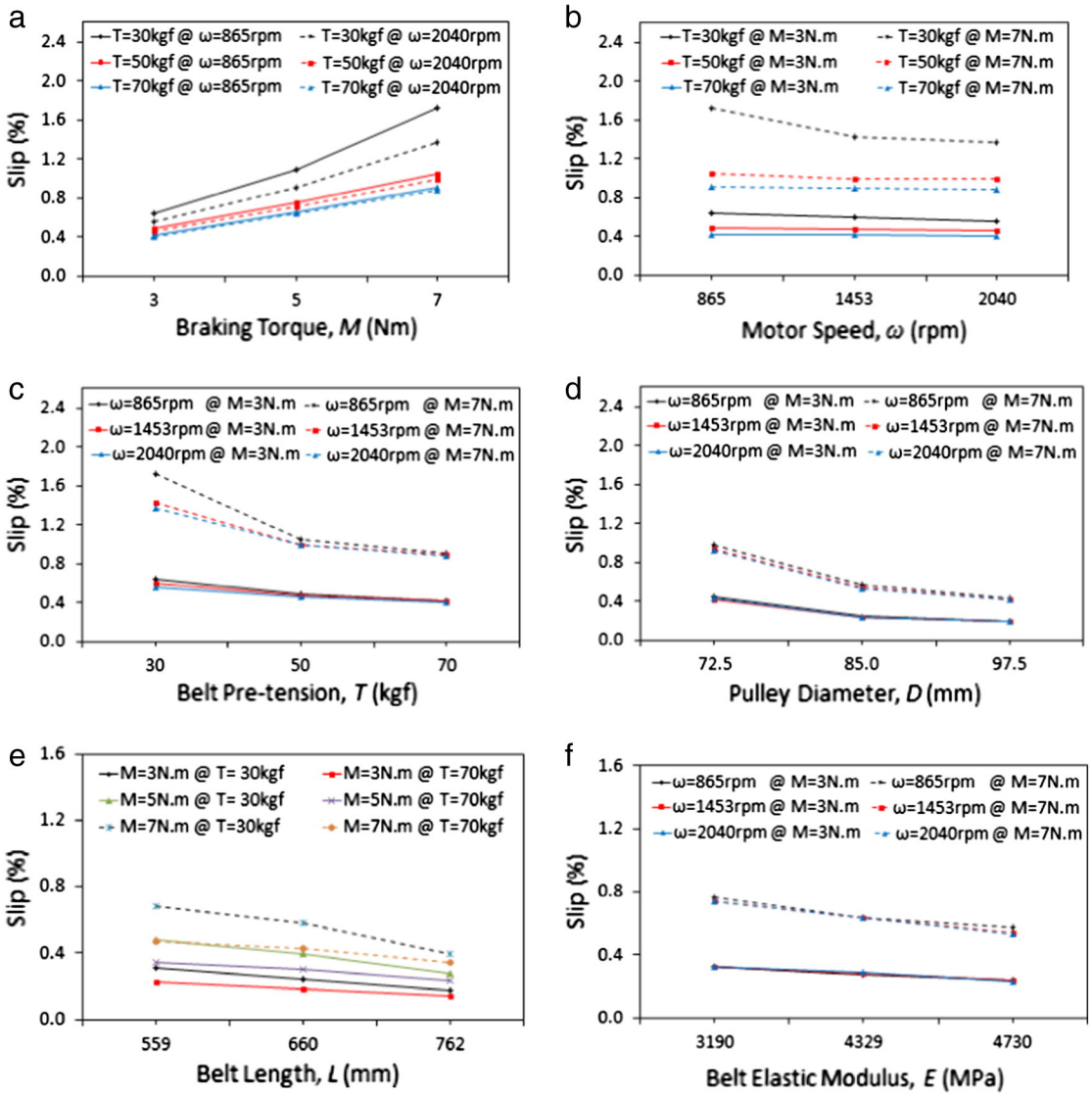

Fig. 4. The relation between % slip and the input parameters: a. Braking torque M, ($E = 3190$ MPa, $L = 559$ mm, $D = 72.5$ mm), b. Driver pulley speed, ω ($E = 3190$ MPa, $L = 559$ mm, $D = 72.5$ mm), c. Belt pre-tension, T, ($E = 3190$ MPa, $L = 559$ mm, $D = 72.5$ mm), d. Pulley diameter, D, ($E = 3190$ MPa, $L = 559$ mm, $T = 50$ kgf), e. Belt length, L, ($E = 4329$ MPa, $\omega = 865$ rpm, $D = 97.5$ mm), and f. Belt elastic modulus, E, ($L = 559$ mm, $T = 50$ kgf, $D = 72.5$ mm).

in input speed, ω_{driver}. As shown in Fig. 4c, the slip behavior is alleviated by higher pre-tension. This effect is more noticeable at high braking torques and low speeds. In Fig. 4d, slip losses are given as a function of pulley diameter. Increasing pulley diameter noticeably reduces the slip. This effect is more pronounced at high levels of braking torque. In Fig. 4e, slip losses are presented as a function of belt length. Slip slightly decreases when longer belts are used; this is more pronounced with high braking torques. As indicated in Fig. 4f, slip loss behavior is improved with the use of stiffer belts. As the results signify, the braking torque is the most dominant factor. Nonlinearities are observed in the relations between % slip and some belt-drive parameters as seen in Fig. 4a–d.

Table 4
The range of values for the design factors used in RSM.

Factor	Unit	High (+1)	Low (−1)
Motor speed, ω	rpm	2040	865
Braking torque, M	Nm	7	3
Belt pre-tension, T	Kgf	70	30
Pulley diameter, D	mm	97.5	72.5
Belt elastic modulus, E	MPa	4730	3190

Table 5
Design matrix.

	Runs	1	2	3	4	5	6	7	8	9	10	11	12	13	14	15
Factor 1	X_1	−1	1	−1	1	−1	1	−1	1	−1	1	−1	1	−1	1	−1
Factor 2	X_2	−1	−1	1	1	−1	−1	1	1	−1	−1	1	1	−1	−1	1
Factor 3	X_3	−1	−1	−1	−1	1	1	1	1	−1	−1	−1	−1	1	1	1
Factor 4	X_4	−1	−1	−1	−1	−1	−1	−1	−1	1	1	1	1	1	1	1
Factor 5	X_5	−1	−1	−1	−1	−1	−1	−1	−1	−1	−1	−1	−1	−1	−1	−1
Response	Slip %	0.546	0.466	[a]	1.144	0.389	0.379	0.848	0.830	0.247	0.228	0.616	0.608	0.190	0.196	0.455

[a] Unavailable data point.

2.5. Experimental study via response surface methodology (RSM)

If a classical test methodology is used like OFAT, in order to reach conclusions similar to that of DoE or RSM, a great number of tests need to be performed; otherwise the conclusions would be incomplete or misleading due to inadequate number of tests or inappropriate test range. Individual effects can be determined using OFAT by varying one parameter and keeping the rest of the parameters the same; however if the interactions between the parameters are important, or testing time and/or resources are limited, then methods like DoE or RSM need to be used [46].

In this study, a response surface method is used to estimate the quantitative relationship between the key controllable variables and response variables. Moreover, RSM is particularly used in cases where several input variables (X_i) potentially influence some performance measure or quality characteristic of the product or process (Y) [47–50]. The quadratic response surface is always described in terms of a second order polynomial as follows [50]:

$$Y = b_0 + \sum_{i=1}^{n} b_i X_i + \sum_{i=1}^{n}\sum_{j=1}^{n} b_{ij} X_i X_j \tag{2}$$

where n is the number of input variables, and b_0, b_i, and b_{ij} represent the coefficients of constant, linear, and quadratic terms, respectively. In order to build the empirical response model, the necessary data are usually collected in accordance with the design of experiments; then single or multiple statistical regression techniques are applied.

In the present study, pulley diameter, belt elastic modulus, brake torque, motor speed, and belt pre-tension are considered as input parameters effective on the slip behavior of V-ribbed belt drives, where % slip is considered as the response parameter. The range of values for each factor is given in Table 4. The upper and lower limits are chosen based on the laboratory experience, physical resources, and on the information published in the scientific literature for similar systems.

The high levels in terms of coded value are set to (+1), and the low ones to (−1). The coded variables are calculated as follows

$$X_1 = \frac{\omega-\omega_0}{\frac{\Delta\omega}{2}},\quad X_2 = \frac{M-M_0}{\frac{\Delta M}{2}},\quad X_3 = \frac{T-T_0}{\frac{\Delta T}{2}}$$
$$X_4 = \frac{D-D_0}{\frac{\Delta D}{2}},\quad X_5 = \frac{E-E_0}{\frac{\Delta E}{2}} \tag{3}$$

where X_i are the coded factors for ω, M, T, D, and E; ω_0, M_0, T_0, D_0, and E_0 are the mean values of the factors; $\Delta\omega$, ΔM, ΔT, ΔD, and ΔE are the differences between the highest and lowest values.

The experiment plan, generated in accordance with the face-centered composite design, consists of 50 runs. The factorial portion is a full factorial design with all combinations of the parameters at two levels and composed of 10 central points and 8 star points. The design matrix and all the corresponding results of % slip are given in Table 5.

2.5.1. RSM results

According to RSM, no statistically significant dependence of % slip on speed is observed. Some of the nonlinearities observed in OFAT tests are found to be statistically insignificant by RSM. As Fig. 5a and b indicate, the relation between % slip and the braking torque or the pre-tension is linear. Fig. 5c reveals a nonlinear inverse relation between % slip and pulley diameter, D. A similar relation for D was also found in earlier studies of V-belts and flat belts [3,5,7,11]. As shown in Fig. 5d, % slip slightly decreases with an increase in the elastic modulus of the belt. One may conjecture that stiffer belts result in lower deformation and thus lower % slip values.

The response surface plot and contour plot of % slip variation under the effects of pre-tension and braking torque are presented in Fig. 6a. The plot indicates that higher pre-tension with lower braking torque results in decrease in % slip. Higher braking torque means a higher level of frictional torque applied to the belt. This results in larger deformation of the belt and thus higher slippage between the belt and the pulley. Considering that the braking torque has a pre-selected value depending on the requirements from the belt drive, it is not considered as a design variable. For this reason, if high breaking torque is required, a higher level of pre-tension needs to be selected to compensate increased speed losses. If the belt in a power transmission system is not tensioned properly to provide sufficient friction between the belt and the pulleys, then slippage occurs and consequently increased power losses. High levels of

16	17	18	19	20	21	22	23	24	25	26	27	28	29	30	31	32
1	−1	1	−1	1	−1	1	−1	1	−1	1	−1	1	−1	1	−1	1
1	−1	−1	1	1	−1	−1	1	1	−1	−1	1	1	−1	−1	1	1
1	−1	−1	−1	−1	1	1	1	1	−1	−1	−1	−1	1	1	1	1
1	−1	−1	−1	−1	−1	−1	−1	−1	1	1	1	1	1	1	1	1
−1	1	1	1	1	1	1	1	1	1	1	1	1	1	1	1	1
0.447	0.426	0.415	1.100	1.100	0.343	0.335	0.769	0.735	0.203	0.192	0.500	0.463	0.170	0.167	0.403	0.373

belt tension, on the other hand, have adverse effects. A high tension increases the pulley hub load, which causes premature failure of the bearings, while a low tension results in slippage. Fig. 6b shows the effects of the pulley diameter and the braking torque on % slip. Use of a larger pulley diameter combined with lower braking torque results in decreased % slip. When the smallest pulley is used and the braking torque takes its maximum value, tension difference between the tight side and the slack side of the belt reaches to its maximum level. Therefore, the change in the extension experienced by the belt during its contact with the pulley will be larger. This leads to a larger creep and thus increased slippage. With smaller pulley sizes, hysteresis losses will also be higher due to a larger change in normal strains and a larger extent of bending and unbending of the belt as it runs over the pulleys. If a high level of braking torque is required, a larger pulley diameter is recommended to reduce the power losses. The plot in Fig. 6c presents interactions of the pulley diameter and the pre-tension in affecting % slip. Smaller pulley diameters together with lower pre-tension result in higher % slip. A similar effect is also observed by Childs and Cowburn [11] in V-belt drives. When the belt tension is low, then, the normal forces between the belt and pulley will not be high enough to generate sufficient frictional forces to sustain the transmission. However, as observed in Fig. 6c, pre-tension does not have a strong effect on % slip in V-ribbed belt drives as long as gross slippage does not occur.

2.5.2. ANOVA

Analysis of variance (ANOVA) is a commonly used statistical method based on decomposition of the total variability in the response variable, *Y*. Using ANOVA, comparisons can be made between the means of two or more parameters in order to differentiate the effective parameters on the desired response. Table 6 presents the statistical significance of each input variable as well as the interaction terms on the % slip behavior. If the value of Prob > F is smaller than 0.05, the regression model is considered to be statistically significant; otherwise the variable does not have a statistically significant effect on the response parameter. Table 6 presents only the significant terms obtained by backward elimination. The main factors, quadratic terms as well as the interaction terms shown in Table 6, have Prob > F values less than 0.05; consequently they are considered to be significant. As indicated In Table 6, there is no significant lack of fit in the model, which is expressed by Eq. (4); so it can be concluded that the reduced model is adequate. The F value of a term reflects the degree of its significance. Highest F values are obtained to be 1642 for the braking torque and 1122 for the pulley diameter. This means that they are the most effective parameters on the response, i.e. % slip.

The quadratic equation of the response surface model of % slip obtained by regression analysis is given in coded parameters by

$$\begin{aligned} Slip\ (\%) = {} & 0.42 + 0.2X_2 - 0.072X_3 - 0.17X_4 - 0.033X_5 - 0.039X_2X_3 - 0.065X_2X_4 \\ & + 0.033X_3X_4 + 0.059X_4^2 + 0.038X_5^2. \end{aligned} \tag{4}$$

Furthermore, the value of R^2 is obtained to be 98.81% for the RSM model. This value indicates that the model will predict future data quite well. R^2 is a measure of the strength of the relationship between the experimental data and the predicted values from the regression model and expressed as

$$R^2 = \frac{SS_R}{SS_T} \tag{5}$$

where SS is the sum of squares; *T* and *R* indicate the total model and regression model, respectively.

3. Optimization of design parameters

3.1. Objective function

After finding the functional relationship between the key controllable variables and the response variable, it is possible to optimize the response. The objective function to be minimized is given in Eq. (4).

3.2. Case study

Speed loss is a critical factor in belt-drive transmissions in which small pulleys are used like front-end accessory drives (FEAD) in automotive vehicles. The optimization problem in this case study is to find the optimal values of the design

Table 5 (*continued*)

	Runs	33	34	35	36	37	38	39	40	41	42	43	44	45	46	47	48	49	50
Factor 1	X_1	−1	1	0	0	0	0	0	0	0	0	0	0	0	0	0	0	0	0
Factor 2	X_2	0	0	−1	1	0	0	0	0	0	0	0	0	0	0	0	0	0	0
Factor 3	X_3	0	0	0	0	−1	1	0	0	0	0	0	0	0	0	0	0	0	0
Factor 4	X_4	0	0	0	0	0	0	−1	1	0	0	0	0	0	0	0	0	0	0
Factor 5	X_5	0	0	0	0	0	0	0	0	−1	1	0	0	0	0	0	0	0	0
Response	Slip %	0.403	0.411	0.251	0.586	0.489	0.385	0.594	0.335	0.500	0.388	0.413	0.413	0.413	0.413	0.413	0.413	0.413	0.413

parameters for minimum % slip for these harsh operating conditions subject to the constraints on the values of the variables. This problem can be stated as

$$\begin{aligned} &\text{Minimize} && F(z) = \%\ \text{slip} \\ &&& F(z) = f(T,\ D,\ E) \\ &\text{Subject to} \\ &&& 30\ \ kgf \le T \le 70\ \ kgf \\ &&& 72.5\ \ mm \le D \le 97.5\ \ mm \\ &&& 3190\ \ MPa \le E \le 4730\ \ MPa \\ &\text{for} && L = 660\ \ mm. \end{aligned} \tag{6}$$

Only the design parameters, pre-tension, elastic modulus, and pulley diameter, are chosen as optimization variables. The same upper and lower limits (Table 4) are used in the design optimization as in the response surface analysis, while the length is taken to be constant. Braking torque and pulley speed levels, on the other hand, depend on the usage of the accessory components (e.g. air conditioning unit) and their operation conditions. Accordingly, their values are not set during the belt drive design. Length of the belt is not found to have a statistically significant effect on % slip. For that reason, in this study, for given levels of braking torque, the other parameters, T, D, and E, are optimized. A typical accessory unit in a FEAD system takes about 3 to 7 N.m load from the

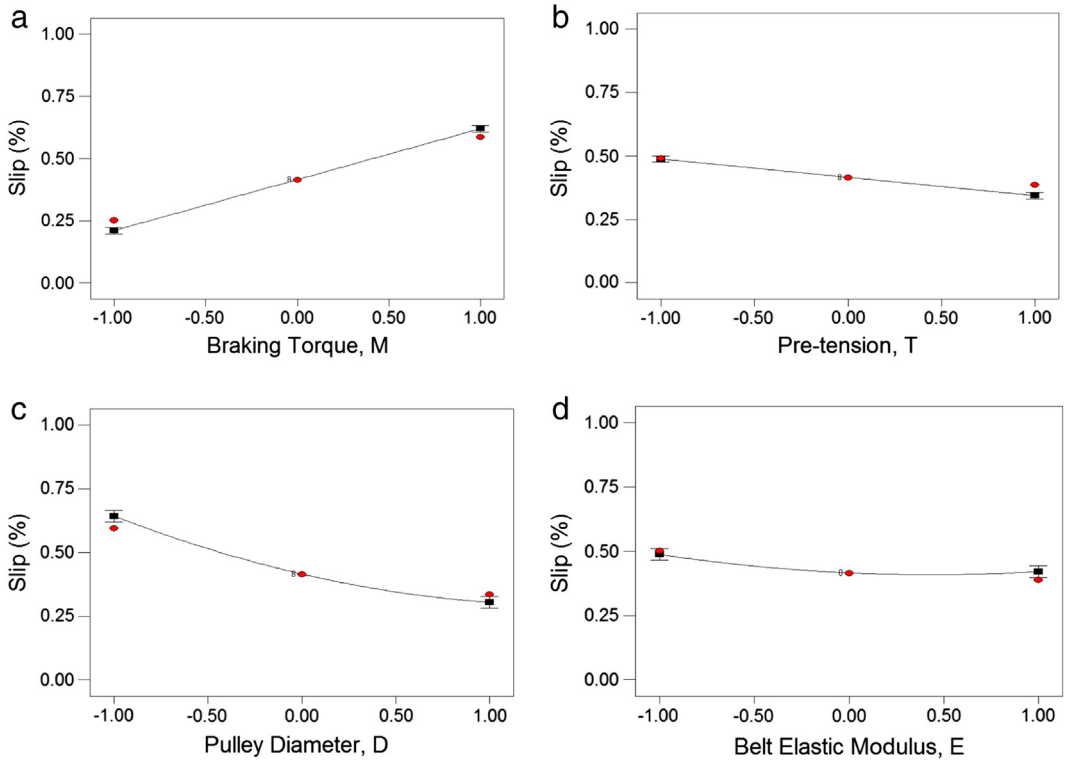

Fig. 5. Individual factor effects on % slip: a. Braking torque, *M*, for $E = 3960$ MPa, $T = 50$ kgf, $D = 85$ mm, b. Pre-tension, *T*, for $M = 5$ N.m, $E = 3960$ MPa, $D = 85$ mm, c. Pulley diameter, *D*, for $M = 5$ N.m, $T = 50$ kgf, $E = 3960$ MPa, and d. Belt elastic modulus, *E*, for $M = 5$ N.m, $T = 50$ kgf, $D = 85$ mm. For all cases, $L = 660$ mm and $\omega = 1453$ rpm.

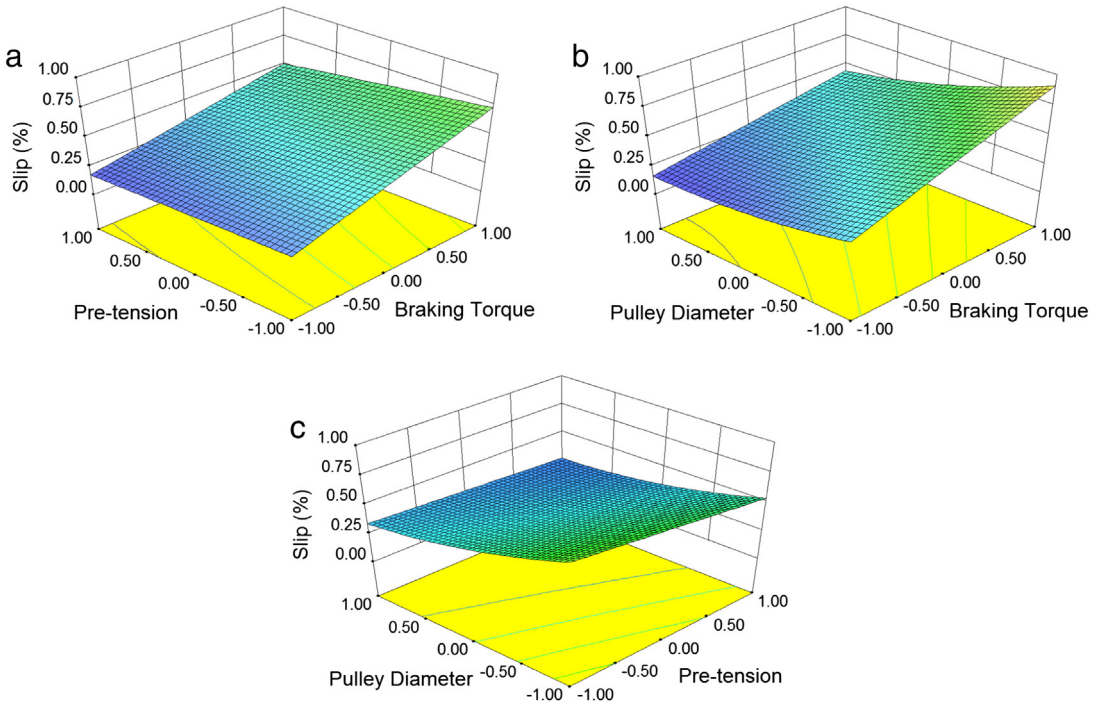

Fig. 6. Response surface and contour plots of % slip variation vs. a. Pre-tension, T, and braking torque, M, for $D = 85$ mm, $E = 3960$ MPa, b. Pulley diameter, D, and braking torque, M, for $T = 50$ kgf, $E = 3960$ MPa, and c. Pulley diameter, D, and pre-tension, T, for $M = 5$ N.m, $E = 3960$ MPa. For all cases, $L = 660$ mm and $\omega = 1453$ rpm.

crankshaft depending on the power requirements. In this case study, the braking torque levels are then chosen within this range. Optimal settings, which minimize % slip within the selected ranges, are listed in Table 7 in terms of coded values. Depending on typical usage of the accessory components, one of the optimum settings may be used in belt drive design.

4. Verification of the model

4.1. Confirmation experiments

In order to verify the response surface model, additional tests are performed using the same experimental setup with arbitrarily chosen values for the belt drive parameters. The confirmation experiments reveal that the difference between the predicted values for % slip and the experimental values are smaller than 7%. One may conclude that the proposed model for % slip in V-ribbed belt drives is reasonably accurate.

Table 6
ANOVA for % slip (after backward elimination).

		Source	Sum of squares	Degree of freedom	Mean square	F value	Prob > F	
		Model	2.5000	9	0.2800	332	<0.0001	Significant
		X_2	1.3700	1	1.3700	1642	<0.0001	
		X_3	0.1700	1	0.1700	204	<0.0001	
		X_4	0.9400	1	0.9400	1122	<0.0001	
		X_5	0.0360	1	0.0360	43	<0.0001	
		$X_2 \cdot X_3$	0.0470	1	0.0470	56	<0.0001	
Std. dev.	0.0290	$X_2 \cdot X_4$	0.1300	1	0.1300	156	<0.0001	
Mean	0.4700	$X_3 \cdot X_4$	0.0330	1	0.0330	39	<0.0001	
C.V. %	6.1700	X_4^2	0.0120	1	0.0120	15	0.0004	
PRESS	0.0570	X_5^2	0.0053	1	0.0053	6	0.0157	
R-squared	0.9881	Residual	0.0330	39	0.0008			
Adj. R-squared	0.9842	Lack of fit	0.0330	32	0.0010			Not significant
Pred. R-squared	0.9776	Pure error	0.0000	7	0.0000			
Adeq. precision	73.4640	Cor. total	2.5300	48				

Table 7
Optimal settings for minimal % slip for given levels of braking torque.

Set levels	Optimal levels			
Braking torque	Pre-tension	Pulley diameter	Elastic modulus	Slip (%)
−1.00	0.99	0.90	0.90	0.16
0.00	1.00	1.00	0.48	0.26
1.00	1.00	1.00	0.44	0.36

4.2. Correlation with the results in the literature

In some of the previous studies, similar belt-drive systems were used and the slip was measured for different test conditions. Table 8 presents % slip values measured by Yu [29] and the predictions of the RSM model given in Eq. (4). The results of the model developed in the present study are in good agreement with the empirical data provided by Yu [29]. The experiments were conducted in that study with the following test conditions: Pulley diameter = 80 mm, motor speed = 1000 rpm, and pre-tension = 42.83 kgf. Because the elastic modulus of the belt used in the experiments was not given in the reference, the medium value is used for the belt elastic modulus in the calculations. The results correlate well even though some of the values of braking torque are outside the limits chosen for the braking torque in the present study.

5. Model adequacy check

In order to ensure that the models have extracted all the relevant information from the experimental data, the adequacy of the experimental design is examined. The residual analysis is the primary diagnostic tool for this purpose [43,44,46]. Residual is defined as the difference between the actual and predicted values of the response for a given design. The results of the residual analysis are shown in Fig. 7a, b, and c.

First of all, for an adequate model, the residuals should have normal distribution regardless of whether the response has a normal distribution or not. The vertical axis of Fig. 7a is the probability scale and the horizontal axis is the data scale. A least-square line is fitted to the plotted points. The line forms an estimate of the cumulative distribution function for the population from which data are drawn. The P-value for the data shown in Fig. 7a is larger than 0.05, thus, the residuals for % slip values follow a normal distribution.

Fig. 7b represents the fitted value plot, where the values of % slip predicted by the response curve are on the horizontal axis and the differences between the actual and predicted values are on the vertical axis. The fitted value plot should represent equal variance levels around the center line, which corresponds to zero residual value, as shown in Fig. 7b.

Fig. 7c represents the order of the data plot, where the data are given in the observed order on the horizontal axis and the residual values are given on the vertical axis similar to the fitted value plot. The measurements should not affect subsequent measurements or the setup should not produce data showing any significant trend over time. The measured data in the present study can be considered to be adequate in this respect. From these figures, one may conclude that the predictive regression model obtained at the final stage of the study is adequate in the sense that the basic assumptions of the regression analysis like errors being uncorrelated are correct.

6. Conclusions

In this study, a test setup is developed to determine the effects of pulley diameter, pulley speed, belt length, belt pre-tension, belt material, and braking torque on % slip (% speed loss) in V-ribbed belt drives. One-factor-at-a-time (OFAT) and response surface test methodologies are used to find the relation between belt-drive parameters and % slip.

Slip measurements on the V-ribbed belt drive system reveal that the smaller is the pulley size, the larger is the belt slip. Experimental analysis shows that below a certain level of belt pre-tension, slip values increase rapidly under all types of test conditions. This may be explained as poor fit between the belt and the pulley grooves. Increasing the braking torque causes a significant increase in slip. This effect is alleviated by high pre-tension. Although the absolute value of slip increases with an increase in driver pulley speed, % slip remains almost constant. When stiffer belts are used, % slip is slightly reduced.

RSM study clearly shows that the belt drive parameters have interactions among themselves and some of the relations between the belt-drive parameters and % slip are nonlinear. Response surface plots distinctly indicate the effective parameters and the nature of their effects on the % slip.

Table 8
The correlation of RSM results with previously reported experimental data.

Braking torque (N.m)	RSM Slip (%)	Yu [29] Slip (%)	Difference (%)
2.5	0.22	0.20	9.1
6.8	0.75	0.70	6.7
10.5	1.20	1.15	4.2

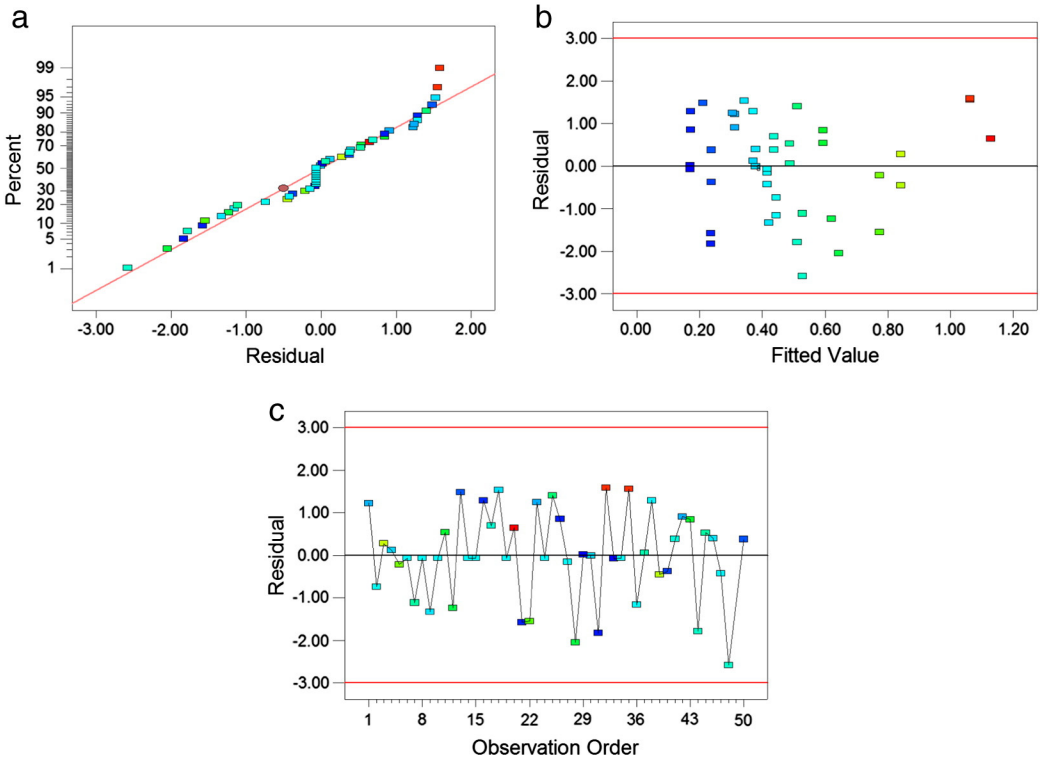

Fig. 7. Adequacy check for the response surface design: a. Normal distribution plot of the residuals, b. Fitted value plot for % slip, and c. Observation order plot of residuals for % slip.

The adequacy of the RSM model is checked and verified via ANOVA. Besides, experiments are conducted with arbitrary operating conditions; then the measured values of % slip and the values predicted by RSM are compared. The comparison indicates that the errors are smaller than 7%. The predictions of the formulation are also found to be in good agreement with the results of a previous experimental study in the literature.

Usually motor speed and braking torque have pre-defined values at the beginning of a belt drive design. In this study, the optimum operating conditions are found for preselected values of braking torque by minimizing the function for % slip derived by RSM.

Acknowledgments

We would like to thank Assoc. Prof. Dr. Mehmet Uçar and Bülent Balta, for their valuable support to this study. We would like to thank Teklas A.Ş. where stiffness measurements are performed.

References

[1] A. Almeida, S. Greenberg, Technology assessment: energy-efficient belt transmissions, Energy Build. 22 (3) (1995) 245–253.
[2] O. Reynolds, On the efficiency of belts or straps as communicators of work, Engineering 38 (1874) 396.
[3] G. Gerbert, On flat belt slip, Veh. Tribol. Ser. 16 (1991) 333–339.
[4] K.L. Johnson, Contact Mechanics, first ed. Cambridge University Press, London, 1987.
[5] T.C. Firbank, Mechanics of the belt drive, Int. J. Mech. Sci. 12 (1970) 1053–1063.
[6] G. Gerbert, Some notes on V-belt drives, J. Mech. Des. 103 (1981) 8–18.
[7] G. Gerbert, Belt slip-a unified approach, J. Mech. Des. 118 (1996) 432s–438s.
[8] F. Sorge, G. Gerbert, Full sliding "adhesive-like" contact of V-belts, ASME J. Mech. Des. 124 (4) (2002) 706–712.
[9] H. Peeken, F. Fischer, Experimental investigation of power loss and operating conditions of statically loaded belt drives, Proceedings of the 1989 International Power Transmission and Gearing Conference, Illinois, 1989, pp. 15–24.
[10] T.H.C. Childs, D. Cowburn, Power transmission losses in V-belt drives, Part 1: mismatched belt and pulley groove wedge angle effects, Proc. Inst. Mech. Eng. D J. Automob. Eng. 201 (1987) 33–40.
[11] T.H.C. Childs, D. Cowburn, Power transmission losses in V-belt drives, Part 2: effects of small pulley radii, Proc. Inst. Mech. Eng. D J. Automob. Eng. 201 (1987) 41–53.
[12] V.A. Lubarda, Determination of the belt force before the gross slip, Mech. Mach. Theory 83 (2015) 31–37.
[13] F. Ferrando, F. Martin, C. Riba, Axial force test and modeling of the V-belt continuously variable transmission for mopeds, J. Mech. Des. 118 (1996) 266–273.
[14] S. Amijma, T. Fujii, H. Matuoka, E. Ikeda, Study on axial force and its distribution for a newly developed block-type CVT belt, Int. J. Veh. Des. 12 (1991) 324–335.
[15] T.F. Chen, D.W. Lee, C.K. Sung, An experimental study on transmission efficiency of a rubber V-belt CVT, Mech. Mach. Theory 33 (1998) 351–363.
[16] S. Akehurst, N.D. Vaughan, D.A. Parker, D. Simmer, Modeling of loss mechanisms in a pushing metal V-belt continuously variable transmission. Part 1: torque losses due to band friction, Proc. Inst. Mech. Eng. D J. Automob. Eng. 218 (11) (2004) 1269–1281.

[17] S. Akehurst, N.D. Vaughan, D.A. Parker, D. Simmer, Modeling of loss mechanisms in a pushing metal V-belt continuously variable transmission. Part 2: pulley deflection losses and total torque loss validation, Proc. Inst. Mech. Eng. D J. Automob. Eng. 218 (11) (2004) 1283–1293.
[18] S. Akehurst, N.D. Vaughan, D.A. Parker, D. Simmer, Modeling of loss mechanisms in a pushing metal V-belt continuously variable transmission. Part 3: belt slip losses, Proc. Inst. Mech. Eng. D J. Automob. Eng. 218 (11) (2004) 1295–1306.
[19] L. Bertini, L. Carmignani, F. Frendo, Analytical model for the power losses in rubber V-belt continuously variable transmission (CVT), Mech. Mach. Theory 78 (2014) 289–306.
[20] G. Mantriota, Theoretical and experimental study of a power split continuously variable transmission system, Part 1, Proc. Inst. Mech. Eng. D J. Automob. Eng. 215 (2001) 837–850.
[21] G. Mantriota, Theoretical and experimental study of a power split continuously variable transmission system, Part 2, Proc. Inst. Mech. Eng. D J. Automob. Eng. 215 (2001) 851–864.
[22] G. Mantriota, Power split continuously variable transmission systems with high efficiency, Proc. Inst. Mech. Eng. D J. Automob. Eng. 215 (2001) 357–368.
[23] G. Mantriota, E. Pennestri, Theoretical and experimental efficiency analysis of multi-degrees-of-freedom epicyclic gear trains, Multi-Body Syst. Dyn. 9 (2003) 389–408.
[24] G. Carbone, L. Mangialardi, B. Bonsen, C. Tursi, P.A. Veenhuizen, CVT dynamics: theory and experiments, Mech. Mach. Theory 42 (2007) 409–428.
[25] G. Carbone, L. Mangialardi, G. Mantriota, The influence of pulley deformations on the shifting mechanism of metal belt CVT, J. Mech. Des. 127 (2005) 103–113.
[26] C. Zhu, H. Liu, J. Tian, W. Xiao, X. Du, Experimental investigation on the efficiency of the pulley-drive CVT, Int. J. Automot. Technol. 11 (2) (2010) 257–261.
[27] K.W. Dalgarno, R.B. Moore, A.J. Day, Tangential slip noise of V-ribbed belts, Proc. Inst. Mech. Eng. C J. Mech. Eng. Sci. 213 (1999) 741–749.
[28] D. Yu, T.H.C. Childs, K.W. Dalgarno, Experimental and finite element studies of the running of V-ribbed belts in pulley grooves, Proc. Inst. Mech. Eng. C J. Mech. Eng. Sci. 212 (1998) 343–355.
[29] D. Yu, Slip of the four belts, Fig. 4.6a, 87(PhD Thesis) Mechanical performance of automotive V-ribbed belts, Department of Mechanical Engineering, The University of Leeds, UK1996.
[30] D. Yu, T.H.C. Childs, K.W. Dalgarno, V-ribbed belt design, wear and traction capacity, Proc. Inst. Mech. Eng. D J. Automob. Eng. 212 (1998) 333–344.
[31] M. Xu, J.B. Castle, Y. Shen, K. Chandrashekhara, Finite element simulation and experimental validation of V-ribbed belt tracking, SAE 2001 World Congress, 2001, 2001. Paper No. 2001-01-0661.
[32] L. Manin, G. Michon, D. Remond, R. Dufour, From transmission error measurement to pulley-belt slip determination in serpentine belt drives: influence of tensioner and belt characteristics, Mech. Mach. Theory 44 (2009) 813–821.
[33] G. Cepon, L. Manin, M. Boltezar, Experimental identification of the contact parameters between a V-ribbed belt and pulley, Mech. Mach. Theory 45 (2010) 1424–1433.
[34] G. Cepon, L. Manin, M. Boltezar, Introduction of damping into the flexible multibody belt-drive model: a numerical and experimental investigation, J. Sound Vib. 324 (2009) 283–296.
[35] G. Cepon, M. Boltezar, An advanced numerical model for dynamic simulations of automotive belt-drives, 2010. SAE 2010-01-1409.
[36] L. Pietra, F. Timpone, Tension in a flat belt transmission: experimental investigation, Mech. Mach. Theory 70 (2013) 129–156.
[37] R.R. Senthilkumar, K. Sooryaprakash, Industrial drive belt tensioning optimization, International Conference on Current Trends in Engineering and Technology, IEEE-32107, ICCTET, 2013, ISBN 978-1-4799-2585-8. 304–306 (Coimbatore, India), IEEE Catalogue Number:CFP1300W-POD.
[38] G. Gerbert, A note on slip in V-belt drives, J. Eng. Ind. Trans. (1976) 1366–1368.
[39] H. Belofsky, On the theory of power transmission by V-belts, Wear 39 (1976) 263–275.
[40] W. Chen, C. Shieh, On angular speed loss analysis of flat belt transmission system by finite element method, Int. J. Comput. Eng. Sci. 4 (2003) 1–18.
[41] S.J. Zhang, Z. Wan, G.L. Liu, Global optimization design method for maximizing the capacity of V-belt drive, Sci. China Technol. Sci. 54 (1) (2010) 140–147.
[42] B. Balta, F.O. Sönmez, A.K. Cengiz, Gage repeatability and reproducibility investigations of a test rig using Anova/Xbar-R method, ASME, International Mechanical Engineering Conference, Paper No. IMECE2011-62130, 3, 2011, pp. 793–800.
[43] F.W. Breyfogle III, Implementing Six Sigma, Smarter Solutions Using Statistical Methods, second ed. John Wiley & Sons, New York, 2003.
[44] The Black Belt Memory Jogger, first ed. GOAL/QPC and SixSigma Academy, 2002.
[45] Measurement System Analysis, Reference Manual, fourth ed. ChryslerGroup LLC, Ford Motor Company, General Motors Corporation, June 2010.
[46] D.C. Montgomery, Design and Analysis of Experiments, fifth ed. Wiley Series in Probability and Statistics, New York, 2001.
[47] C. Chen, P. Su, Y. Lin, Analysis and modeling of effective parameters for dimension shrinkage variation of injection molded part with thin shell feature using response surface methodology, Int. J. Adv. Manuf. Technol. 45 (2009) 1087–1095.
[48] U. Reisgen, M. Schleser, O. Mokrov, E. Ahmed, Statistical modeling of laser welding of DP/TRIP steel sheets, Opt. Laser Technol. 44 (2012) 92–101.
[49] U. Reisgen, M. Schleser, O. Mokrov, E. Ahmed, Optimization of laser welding of DP/TRIP steel sheets using statistical approach, Opt. Laser Technol. 44 (2012) 255–262.
[50] R.H. Myers, D.C. Montgomery, Response Surface Methodology, second ed. Wiley Series in Probability and Statistics, New York, 2002.